Wind and Structures, *Vol. 16, No. 5 (2013) 457-476*
DOI: http://dx.doi.org/10.12989/was.2013.16.5.457

Vortex excitation model. Part I. mathematical description and numerical implementation

T. Lipecki*[1] and A. Flaga[2]

[1]*Faculty of Civil Engineering and Architecture, Lublin University of Technology, Lublin, Poland*
[2]*Wind Engineering Laboratory, Cracow University of Technology, Cracow, Poland*

(Received March 27, 2012, Revised June 6, 2012, Accepted June 20, 2012)

Abstract. This paper presents theoretical background for a semi-empirical, mathematical model of critical vortex excitation of slender structures of compact cross-sections. The model can be applied to slender tower-like structures (chimneys, towers), and to slender elements of structures (masts, pylons, cables). Many empirical formulas describing across-wind load at vortex excitation depending on several flow parameters, Reynolds number range, structure geometry and lock-in phenomenon can be found in literature. The aim of this paper is to demonstrate mathematical background of the vortex excitation model for a theoretical case of the structure section. Extrapolation of the mathematical model for the application to real structures is also presented. Considerations are devoted to various cases of wind flow (steady and unsteady), ranges of Reynolds number and lateral vibrations of structures or their absence. Numerical implementation of the model with application to real structures is also proposed.

Keywords: across-wind load, vortex excitation, lateral vibrations, sectional model, circular cross-section

1. Introduction

Many mathematical models in the field of vortex excitation have been elaborated. Recent improvements of existing models and new approaches were presented by Clobes *et al.* (2011), Verboom and van Koten (2010), Arunachalam (2011). Some aspects of vortex excitation for steel chimneys were also considered by Tranvik and Alpsten (2005), Homma *et al.* (2009), Repetto (2011) or Belver *et al.* (2012). From the point of view of vortex shedding physical description, the semi-empirical model presented in this paper is – in authors' opinion – more exact in comparison to other models that can be found in the literature. The basis of the model is created for a simple case of steady wind flow and for a sectional model of the motionless structure (Flaga 1996, 1997). The fundamental model equations are extrapolated to the real situation when the case of unsteady wind flow always appears for strong winds, and when the analysed structure vibrates laterally. In order to represent the real situation it is necessary to consider random variations of relevant parameters in both space and time. The model can represent the behaviour of slender structures with circular cross-section with constant or varying diameter.

∗Corresponding author, Ph.D., E-mail: t.lipecki@pollub.pl

http://www.techno-press.org/?journal=was&subpage=8 ISSN: 1226-6116 (Print), 1598-6225 (Online)

Various aspects and development of the model were presented in some papers by: Flaga and Lipecki (2005, 2010).

2. Sectional model of the structure

Mathematical equations were developed for a physical model of a system which was an undeformable cylinder supported elastically (including damping) on the ends (i.e., sectional model of the structure – comp. Fig. 1). The following indexes were introduced to clarify notations of next equations: *y* – lateral to the wind direction, *o* – motionless structure, *v* – vibrating structure, *c* – critical vortex excitation, *e* – effective (dimension), $\wedge$ – non-dimensional value. Moreover, non-dimensional wind flow parameters, such as: *Re* – Reynolds number and α_w – mean angle of wind attack are marked as *W* (i.e., $(W) = (Re,\ \alpha_w)$) and non-dimensional structure geometry parameters, such as: *K* – cross-section shape, k_L – structure slenderness, k_B – cross-section slenderness, k_s – equivalent surface roughness are marked as *G* (i.e., $(G)=(K, k_L, k_B, k_s)$).

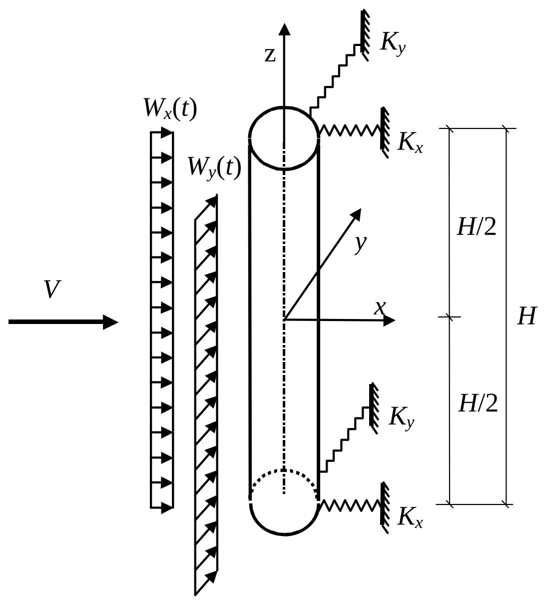

Fig. 1. Assumed physical model of the system

2.1. Case of steady air onflow and motionless structure

A. Subcritical ($Re < (1.0\text{-}1.4)10^5$) and transcritical ($Re > (3.5\text{-}5.0)10^6$) *Re* ranges.

Periodical or quasi-periodical vortex shedding can appear in subcritical or transcritical Reynolds number ranges. Mathematical model of vortex excitation $w_y^o(t)$ (given in N/m) can be described by the relation

$$w_y^o(t) = \frac{1}{2}\rho V^2 D C_y^o \left(\sin 2\pi f^o t + \varphi^o\right) = qD\hat{w}_y^o(t) \tag{1}$$

where: t –time, ρ – air density, V – wind speed, D – characteristic dimension of the cross-section (for circular cylinders – diameter), C_y^o – aerodynamic coefficient of the lift force caused by vortices, $f^{\,o}$ – Strouhal frequency of vortex shedding, $\varphi^{\,o}$ – phase shift angle, $\hat{w}_y^o(t)$ – non-dimensional vortex excitation. In general, values of C_y^o and $f^{\,o}$ for motionless structure depend on W and G parameters.

B. Critical ((1.0-1.4)10^5 < Re < (3.5-5.0)10^5) and supercritical ((3.5-5.0)10^5< Re < (3.5-5.0)10^6) Re ranges.

Vortex shedding in Re regime is intermittent in nature. The mathematical model is very similar to the model in case of unsteady onflow (see 2.3). Frequency $f^{\,o}$ can be treated as frequency at the maximum of power spectral density function of vortex excitation.

2.2. Case of steady air onflow and lateral vibrations of the structure

A. Subcritical and transcritical Re ranges.

The influence of lateral vibrations on vortex excitation can be neglected when the vibration amplitude level is less than 0.01D (Kwok and Melbourne 1980, Vickery and Basu 1983, Basu and Vickery 1983). When the amplitude exceeds that level, strong feedback between lateral vibrations and vortex excitation can appear. One of the major effects of such feedback is the synchronization of frequencies of vortex shedding and natural lateral vibrations of the structure (lock-in phenomenon). Kármán vortices are reinforced by the motion in the lock-in range, so, lateral force can increase significantly. On the basis of several experiments (e.g., Stansby 1976) it can be stated that the amplitude of lateral vibrations increases for wind speed V greater than 0.9V_c^o (V_c^o – critical wind speed for motionless cylinder), it achieves maximum for V in the range (1.2-1.3) V_c^o, and finally, disappears for V above 1.6V_c^o. The case of critical vortex excitation (in lock-in range) can be dangerous for the structure because it can develop resonant vibrations and will be described in more detail. The value of effective lateral dimension D_c^e of the vibrating cylinder is higher than characteristic dimension D for the motionless cylinder. Effective dimension could be connected with the width of the vortex street h_c^v. It can be written

$$D_c^e / D = h_c^v / h^o = 1 + \alpha_c^v \left(A_{\eta_c^v} / D\right) = 1 + \alpha_c^v A_{\hat{\eta}_c^v} \tag{2}$$

where: h_c^v and h^o – width of the vortex street for vibrating and motionless cylinder respectively, $A_{\eta_c^v}, A_{\hat{\eta}_c^v}$ – dimensional and non-dimensional vibration amplitude, α_c^v – experimental parameter of the value in the range 0.7-1.54. The limits of α_c^v can be derived from

1. Sachs (1978) gives the relationship

$$h_c^v / h^o = \left(h^o + 2A_{\eta_c^v}\right) / h^o = 1 + 2A_{\eta_c^v} / h^o \tag{3}$$

For subcritical range of *Re* it can be assumed that $h^o \approx 1.3D$, then

$$D_c^e / D = h_c^v / h^o = 1 + 2A_{\eta_c^v} / \left(1.3D\right) = 1 + 1.54A_{\hat{\eta}_c^v} \quad \rightarrow \quad \alpha_c^v = 1.54 \tag{4}$$

2. According to dimensional analysis the effective dimension $D_c^e \cong \left(D + A_{\eta_c^v}\right)$ should be the characteristic dimension for vortices of one row, then it could be written

$$D_c^e / D = \left(D + A_{\eta_c^e}\right) / D = 1 + 1.0A_{\hat{\eta}_c^e} \quad \rightarrow \quad \alpha = 1.0 \tag{5}$$

3. Finally, on the basis of experiments conducted in subcritical range of *Re* (e.g., Griffin and Ramberg 1974) is

$$D_c^e / D = h_c^v / h^o \cong 1 + 0.7A_{\hat{\eta}_c^v} \quad \rightarrow \quad \alpha_c^v = 0.7 \tag{6}$$

As the first assumption it is reasonable to assume α_v^c as equal to 1.0.

Taking into consideration the effective dimension D_c^e, other value of critical wind speed for vibrating cylinder is obtained

$$V_c^v / V_c^o = D_c^e / D = 1 + \alpha_c^v A_{\hat{\eta}_c^v} \tag{7}$$

Mathematical model of critical vortex excitation at lock-in can be given by

$$\begin{aligned} w_{yc}^v\left(t, A_{\hat{\eta}_c^v}\right) &= q_c^v D_c^e C_{yc}^v \sin\left(2\pi\ f_i t + \varphi_c^v\right) = q_c^o D\left(1 + \alpha_c^v A_{\hat{\eta}_c^v}\right)^3 C_{yc}^v \sin\left(2\pi\ f_i\right) = \\ &= q_c^o D \hat{w}_{yc}^v\left(t, A_{\hat{\eta}_c^v}\right) \end{aligned}$$

where

$$\hat{w}_{yc}^v(t, A_{\hat{\eta}_c^v}) = (1 + \alpha_c^v A_{\hat{\eta}_c^v})^3 C_{yc}^v \sin(2\pi f t \varphi_c^v) = (1 + \alpha_c^v A_{\hat{\eta}_c^v})^3 \hat{w}_{yc}^{v*}(t) \tag{8}$$

and C_{yc}^v – aerodynamic coefficient for a vibrating cylinder that can be assumed as equal to appropriate coefficient for a motionless cylinder.

For the analysed physical model of the system (sectional model), the amplitude of vibrations is described by

$$A_{\hat{\eta}_c^v} = \frac{q_c^o C_{yc}^v}{2\gamma m \omega_i^2}(1 + \alpha_c^v A_{\hat{\eta}_c^v})^3, \frac{A_{\hat{\eta}_c^v}}{(1 + \alpha_c^v A_{\hat{\eta}_c^v})^3} = \frac{q_c^o C_{yc}^v}{2\gamma m \omega_i^2} \tag{9}$$

where: $\omega_i = 2\pi f_i$, γ – coefficient of critical damping ($\gamma = \Delta/2\pi$, Δ – logarithmic decrement of vibrations damping), m – mass per structural unit length. This is a non-linear equation for determining $A_{\hat{\eta}_c^v}$. The function $A_{\hat{\eta}_c^v}/(1+\alpha_c^v A_{\hat{\eta}_c^v})^3$ has the extreme at value $0.148/\alpha_c^v$ for $A_{\hat{\eta}_c^v} = 0.5/\alpha_c^v$. Then $A_{\hat{\eta}_c^v} < A_{\max} = 0.5D/\alpha_c^v$. This means that in the assumed model of across-wind load the feedback between cylinder vibrations and vortex shedding is of self-limited character, which is confirmed by experimental investigation results.

B. Critical and supercritical *Re* ranges.

In this case the feedback between vortices and vibrations can also appear but in general it is much weaker. The frequency of synchronization should be related to the central frequency of the power spectral density function of vortex shedding. Amplitude-frequency characteristics of the random process change from a broad-band process to a narrow-band Gaussian process with extreme value for $f = f_i$.

2.3. Case of unsteady air onflow and motionless structure

On the basis of numerous full-scale measurements and wind tunnel tests some general remarks concerning vortex excitation in turbulent onflow can be formulated:

1. Across-wind action generated by vortices depends on I_v – intensity of turbulence, and L_v – scale of turbulence, and obviously other *W* and *G* parameters.

2. Vortex street parameters are of random character and should be connected with such wind speed that allows considerations of spatial dimensions of the phenomenon. It could be the mean wind speed $V_m(z,t)$, spatially averaged in the distance equal to the dimension $D(z)$ in front of the structure and in the domain $\Delta y(z) = \chi(z)D(z)$ normally orientated with respect to the wind. Parameter $\chi(z)$ for circular cross-section is the number of order 3, and then $\chi(z)D(z)$ is the width of the disturbances in wind field caused by the structure (see Fig. 2).

3. Strong fluctuations of the wind direction appear. In case of circular cylinders the across-wind action caused by fluctuations can be comparable with vortex excitation. Lack of separation between these various actions leads to significant diversity of results obtained in wind tunnel and full-scale measurements.

Mathematical model of vortex excitation can be given by

$$\begin{aligned} w_y^o(z,t) &= \frac{1}{2}\rho V_m^2(z,t) D C_{y1}^o \sin\left(2\pi\ f^o(z,t)t + \varphi^o(z)\right) = \\ &= \frac{1}{2}\rho V^2 D \left(\frac{V_{m(z,t)}}{V}\right)^2 C_{y1}^o C_{y2}^o(z,t) \sin\left(2\pi\ \bar{f}^o t + \varphi^o\right) = \\ & qDC_y^o(z,t)\sin\left(2\pi\ \bar{f}^o t + \varphi^o\right) = qD\hat{w}_y^o(z,t) \end{aligned} \tag{10}$$

where: z – axial coordinate of the cylinder, $C_y^o(z,t)$ – time dependent aerodynamic coefficient of across-wind load caused by vortices

$$C_y^o(z,t) = \left(\frac{V_m(z,t)}{V}\right)^2 C_{y1}^o C_{y2}^o(z,t) \tag{11}$$

$\overline{f}^{o}, \varphi^{o}$ – mean frequency averaged in time domain and phase shift angle averaged in space. Moreover, $C_y^o(z,t)$ and $\overline{f}^{o}$ depend on parameters W, I_v, L_v and G. Non-dimensional vortex excitation $\hat{w}_y^o(z,t)$ is a stochastic process of more or less narrow-band character. The power spectral density function of this process can be with good approximation given in the generalized form (similar to one proposed by Vickery and Clark 1972)

$$\frac{fG_{\hat{w}_y^o}(f)}{\sigma^2_{\hat{w}_y^o}} = \frac{1}{\sqrt{\pi}B^o}\frac{f}{\overline{f}^{o}}\exp\left[-\left(\frac{1-f/\overline{f}^{o}}{B^o}\right)^2\right] \tag{12}$$

where: $\sigma_{\hat{w}_y^o}$ – standard deviation of vortex excitation, B^o – non-dimensional bandwidth parameter. Both parameters strongly depend on turbulence intensity I_v and Re (particularly in the case of circular cylinders).

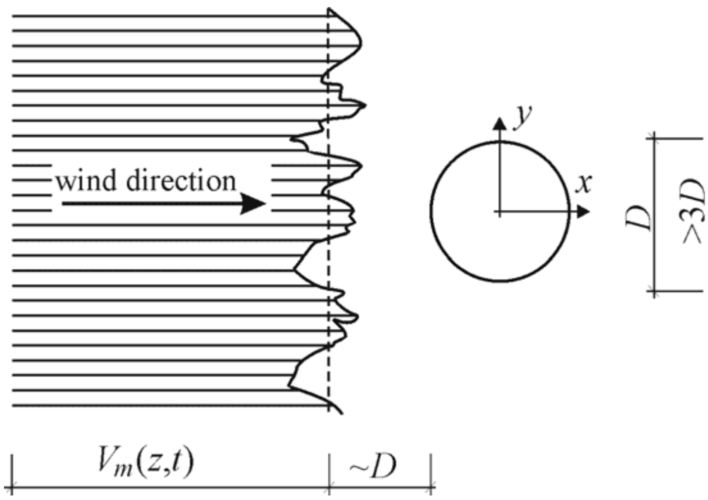

Fig. 2 The way of assuming V_m(z,t)

2.4. Case of unsteady air onflow and vibrating structure

In spite of the fact that vortex shedding is of random character it is controlled by more or less narrow-band random lateral vibrations of the cylinder. Taking into account the narrow-band character of lateral vibrations

$$\eta_c^v(t) = A_{\eta_c^v}(t)\sin\left(2\pi f_i t + \varphi_c^v\right) \tag{13}$$

the effective lateral dimension can be expressed by

$$D_c^e(t)/D = 1+\tilde{\alpha}_c^v(\tilde{A}_{\eta_c^v}(t)/D) = 1+\tilde{\alpha}_c^v\tilde{A}_{\hat{\eta}_c^v}(t) \cong 1+\overline{\alpha}_c^v\sigma_{\eta_c^v}/D = 1+\overline{\alpha}_c^v\sigma_{\hat{\eta}_c^v} \tag{14}$$

where: $A_{\eta_c^v}(t), \tilde{A}_{\hat{\eta}_c^v}(t)$ – time dependent amplitude and averaged in time domain amplitude of vibrations respectively, $\sigma_{\eta_c^v}$ – standard deviation of the response $\eta_c^v(t)$, $\tilde{\alpha}, \overline{\alpha}$ – experimental parameters that depend on parameters W, I_v, L_v and G, and approximately: $\tilde{\alpha} = \overline{\alpha}/\sqrt{2}$. For exact definition of the vortex excitation distribution along the height (or span) of the structure, it is necessary to determine its space correlation function $\rho_{\hat{w}_{yc}^v}$ and length correlation scale $L_{\hat{w}_{yc}^v}$.

Critical vortex excitation can be with good approximation described by the equation

$$\begin{aligned}
w_{yc}^v(z,t) &= \frac{1}{2}\rho\left[V_{mc}^v(z,t)\right]^2 D_c^e C_{yc}^{v*}(z,t)\sin(2\pi f_i t+\varphi_c^v) = \\
&= \frac{1}{2}\rho(V_c^o)^2\left(\frac{V_c^v}{V_c^o}\right)^2\left[\frac{V_{mc}^v(z,t)}{V_c^v}\right]^2\left(1+\overline{\alpha}_c^v\sigma_{\hat{\eta}_c^v}\right)^\beta DC_{yc}^{v*}(z,t)\sin\left(2\pi f_i t+\varphi_c^v\right) = \\
&= q_c^o D\left(1+\overline{\alpha}_c^v\sigma_{\hat{\eta}_c^v}\right)^\beta C_{yc}^v(z,t)\sin\left(2\pi f_i t+\varphi_c^v\right) = \\
&= q_c^o D\left(1+\overline{\alpha}_c^v\sigma_{\hat{\eta}_c^v}\right)^\beta \hat{w}_{yc}^{v*}(z,t) = q_c^o D\hat{w}_{yc}^v\left(z,\sigma_{\hat{\eta}_c^v},t\right),
\end{aligned}$$

$$C_{yc}^v(z,t) = \left[\frac{V_{mc}^v(z,t)}{V_c^v}\right]^2 C_{yc}^{v*}(z,t)$$

$$\hat{w}_{yc}^{v*}(z,t) = C_{yc}^v(z,t)\sin\left(2\pi f_i t+\varphi_c^v\right)$$

$$\hat{w}_{yc}^v\left(z,\sigma_{\hat{\eta}_c^v},t\right) = \left(1+\overline{\alpha}_c^v\sigma_{\hat{\eta}_c^v}\right)^\beta \hat{w}_{yc}^{v*}(z,t) \tag{15}$$

In the above equations $C_{yc}^v(z,t)$ – is the aerodynamic coefficient that depends on W, I_v, L_v and G, $\hat{w}_{yc}^{v*}(z,t)$ – is the narrow-band stochastic process of Gaussian character. The correlation of the process along structure height (or span) depends on W, I_v, L_v and G parameters, and moreover on amplitudes level. The power spectral density function of the process can be described by the relationship (comp. Vickery and Clark 1972)

$$\frac{fG_{\hat{w}_{yc}^{v*}}(f)}{\sigma^2_{\hat{w}_{yc}^{v*}}} = \frac{k_c^{v*}}{\sqrt{\pi}B_c^{v*}}\frac{f}{f_i}\exp\left[-\left(\frac{1-f/f_i}{B_c^{v*}}\right)^2\right] \tag{16}$$

where $\sigma_{\hat{w}_{yc}^{v*}}, B_c^{v*}, k_c^{v*}$ – experimental parameters that depend on W, I_v, L_v and G. The value of k_c^{v*} should be less than 1.0 (its exact meaning is explained in chapter 3.2). A value of $\sigma_{\hat{w}_{yc}^{v*}}$ is similar (slightly higher) to a respective value for motionless structure. A value of B_c^{v*} is lower than a respective value for motionless structure.

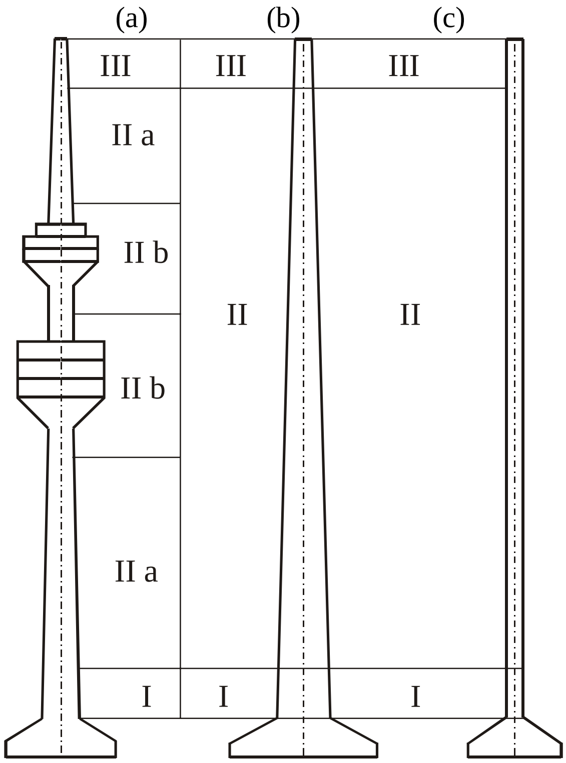

Fig. 3 Zones of vortex excitation along the height of the slender structure for various cross-sections: (a) strongly changeable diameter, (b) tapered diameter and (c) constant diameter

3. Real structure

3.1 Semi-deterministic description

Several factors influence significantly the flow around real structure:

1. Vortex excitation cannot appear in the zones of large flow disturbances caused by boundary zones of the structure (top and base) and significant changes in cross-section shape along the height or span. Sample zones of possible vortex excitations for different types of slender structures are presented in Fig. 3. Zones III and I denote disturbance zones at the top and base of the structure where vortex shedding cannot appear because of 3-D character of the flow around the free end and additional flow turbulence caused by ground surface roughness at the base. Zone IIb is a zone of large disturbances caused by considerable changes in the cross-section shape. In the zone IIb

vortex shedding cannot appear either. Zones IIa and II are the limited regions where vortex excitation is possible.

2. Critical vortex excitation can appear only at the height (or span) of the structure where both profiles of mean wind speed and critical wind speed are close to each other. It is assumed that lock-in could happen in the range $0.9V_c(z) < V_m(z) < 1.3V_c(z)$ (comp. chapter 2.2).

3. Amplitude of lateral vibrations is varying along the height (or span) of the structure according to the ***i***-th mode shape $\Phi_i(z)$.

Due to the fact that exact determination of the spatial distribution of vortex excitation can be difficult in engineering practice, it is proposed considering equivalent vortex excitation process. The equivalent process is time dependent but uniformly distributed along height (or span) of the structure. All experimental parameters describing equivalent process are devoted to the central point z_0 of the domain ΔL. Finally, spatial distribution of the equivalent process is described by 3 deterministic functions $\Theta_i(z)$ of zero-one character.

$\Theta_1(z)$ is the function of disturbances caused by boundary zones and cross-section variations. It is assumed that vortex excitation is possible in zones II and IIa. The dimensions of disturbance zones I and III are equal to the value of the local cross-section diameter $D(z)$. Moreover, vortex shedding can appear at the distance equal to local $D(z)$ from the zone IIb. Function $\Theta_1(z)$ is equal to 1.0 in vortex excitation zones and 0 in other ranges of the structure. There are examples of the function $\Theta_1(z)$ for different types of cantilever structures in Fig. 4.

$\Theta_2(z)$ is the function of accordance between wind speed profile and critical wind speed profile. On the basis of collected data it is assumed that in the range of profiles consistency: $0.9V_c(z) < V_m(z) < 1.3V_c(z)$ vortex excitation can appear. So, the function $\Theta_2(z)$ is equal to 1.0 in this region, whereas in other ranges of the structures it is equal to 0. The way of assuming $\Theta_2(z)$ is presented in Fig. 5.

$\Theta_3(z)$ is the function of the mode shape that defines the direction of the load caused by vortex excitation. Its value is equal to ±1.0 at the whole height (span) and changes the sign in the point where ***i***-th mode shape $\Phi_i(z)$ changes its sign. Sample functions $\Theta_3(z)$ for various kinds of supporting are presented in Fig. 6.

The product of $\Theta_i(z)$

$$\prod \Theta_i(z) = \Theta_1(z)\Theta_1(z)\Theta_3(z) \tag{17}$$

defines zone (or zones) L_1 of the structure where vortex excitation can appear.

The product function $\prod \Theta_i(z)$ is modified to the function $\Theta(z)$ taking into account the influence of vibration amplitude variations along the structure. Such modification should be carried out according to the following rules: (1) the area of the new, zero-one function $\Theta(z)$ of the new length L_2 is equal to the area under the curve of the mode shape $\Phi_i(z)$ in the domain given by function $\prod \Theta_i(z)$ of the length L_1, (2) new domain of the length L_2 of the function $\Theta(z)$ is referred to the maximum value of $\Phi_i(z)$ in this region (see Fig. 8). The function of the mode shape is normalized to 1.0 in the point of maximum deflection.

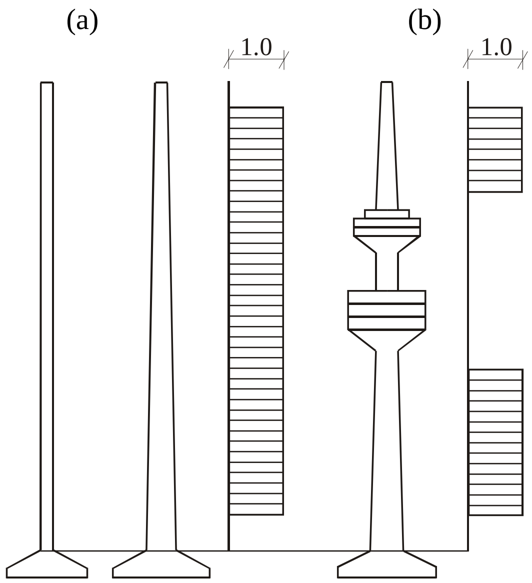

Fig. 4 Function $\Theta_1(z)$ for different kinds of cross-sections: (a) constant or tapered and (b) strongly changeable

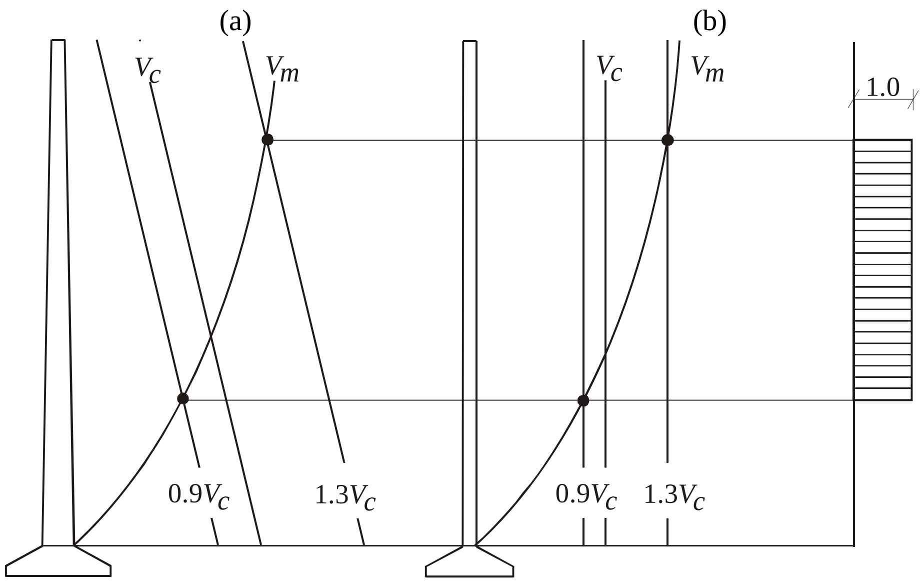

Fig. 5 Function $\Theta_2(z)$ for different kinds of cross-sections: (a) tapered and (b) constant

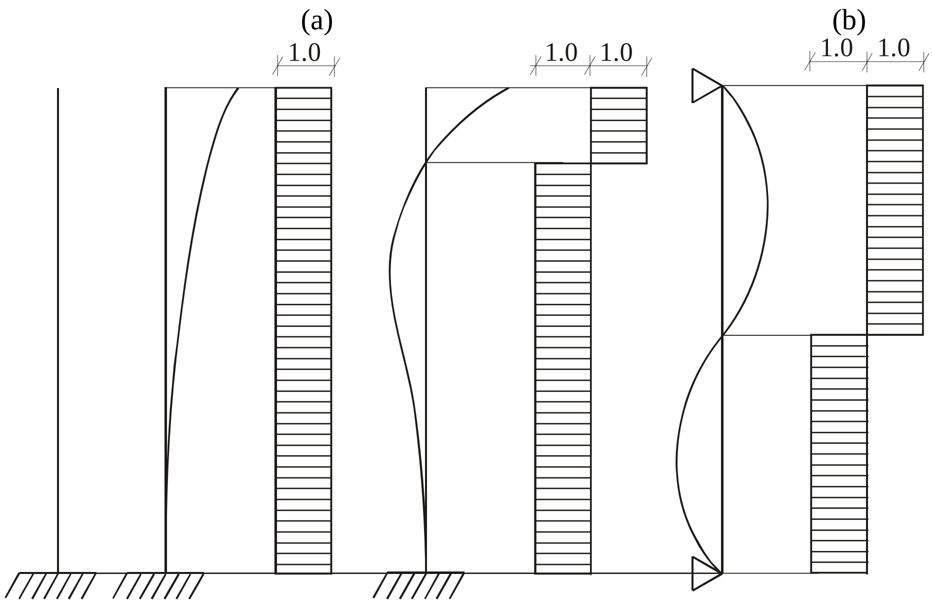

Fig. 6 Function $\Theta_3(z)$ in two cases of static schemes: (a) cantilevered structure, the 1st and the 2nd mode and (b) simple supported structure, the 2nd mode

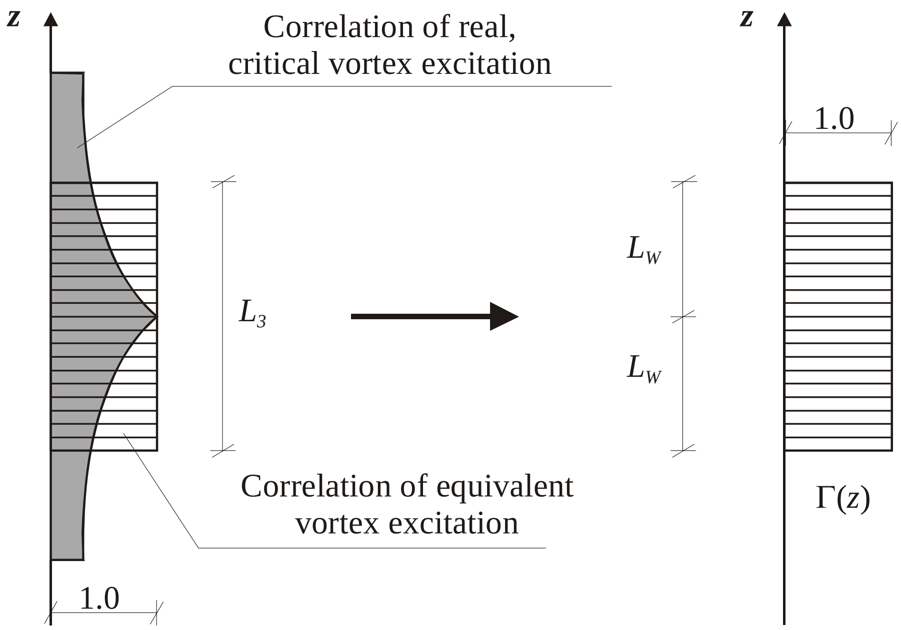

Fig. 7 Deterministic function $\Gamma(z)$

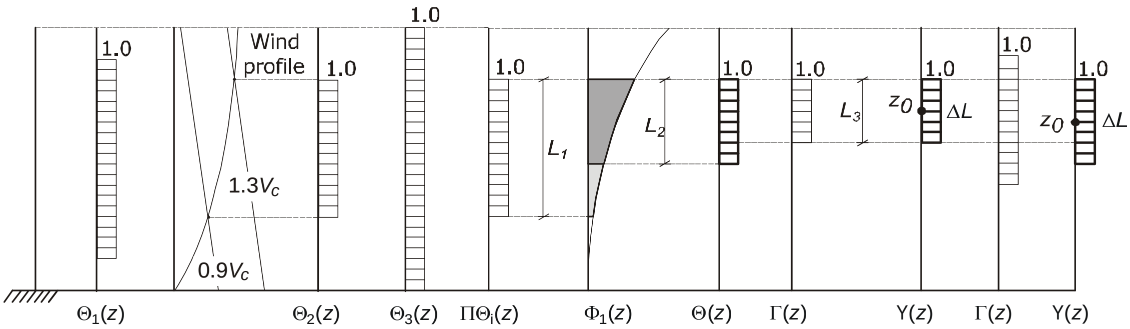

Fig. 8 Procedure of assuming the zero-one function *Y(z)*, and domain ΔL with its central point z_0 for a cantilever structure

Critical vortex excitation is a stochastic process both in space and time, so the space-time correlation of the process should be determined. In order to simplify the mathematical model for engineering use it can be assumed that vortex excitation is a stochastic process in time and has uniform distribution along the height (or span) of the structure in the domain defined by function $\Theta(z)$. It means that the process is fully correlated in vortex shedding domain. Taking that into account next deterministic, zero-one function $\Gamma(z)$ is introduced. Function $\Gamma(z)$ is connected with normalised space correlation function of the real, critical vortex excitation, and defines domain L_3 where the process is fully correlated. Such assumption allows to replace the real, critical vortex excitation with equivalent load of the simple rectangular distribution (Fig. 7). It can be assumed that the domain L_3 of the function $\Gamma(z)$ is equal to $2L_{\hat{w}}$, where $L_{\hat{w}}$ is a non-dimensional correlation length scale.

The final function $Y(z)$ is the product of zero-one functions $\Theta(z)$ and $\Gamma(z)$. Function $Y(z)$ defines zone (zones) ΔL of vortex excitation and its central (characteristic) point z_0.

The whole deterministic procedure can be summarized in the following points: 1. Determination of $\Theta_i(z)$ and domain L_1. 2. Calculation of $\Theta(z)$ and domain L_2. 3. Determination of $\Gamma(z)$ and domain L_3. 4. Calculation of the final function $Y(z) = \Theta(z)\Gamma(z)$ and domain ΔL. The procedure is presented schematically for cantilever structure in Fig. 8. There are two possible cases of relation between functions $\Theta(z)$ and $\Gamma(z)$: $\Theta(z)<\Gamma(z)$ and $\Theta(z)>\Gamma(z)$ in Fig. 8.

3.2. Mathematical model of critical vortex excitation

Equations of the mathematical model elaborated in chapter 2 were extrapolated to applications for real slender structures. All considerations are related to equivalent process in domain ΔL, and all experimental parameters are related to point z_0. Critical vortex excitation for unsteady wind flow and laterally vibrating slender structure can be given with a good approximation by the following formula (indexes c – critical and v – vibrating structure are omitted in subsequent equations)

$$w_y(t) = \left[q_c \cdot D \cdot (1+\alpha \cdot \sigma_{\hat{\eta}})^3 \cdot \hat{w}_y(t) \right]\Big|_{z=z_0} \cdot Y(z) \tag{18}$$

where: z – co-ordinate (height, span); t – time; $q_c = 0.5\rho V_c^2$ – pressure of critical wind speed V_c; D – characteristic cross-section dimension in point z_0; α – parameter describing increase in effective cross-section diameter (experimental value); $\sigma_{\hat{\eta}}$ – standard deviation of structure response under critical vortex excitation (given in non-dimensional displacements); $\left(1+\alpha\cdot\sigma_{\hat{\eta}}\right)^3$ – factor that takes into account increase in effective cross-section diameter of the laterally vibrating structure, so diameter D is amplified during vibrations; $Y(z)$ – deterministic function that describes zone (or zones) along the height (or span) of the structure ΔL, where vortex excitation can appear; z_0 – central point of the domain ΔL, $\hat{w}_y(t)$ – non-dimensional vortex excitation described by formula

$$\hat{w}_y(z,t) = \left[\left[\frac{V_m(z,t)}{V_c}\right]^2 C_y(z,t)\cdot\sin\left(2\pi f_i t+\varphi\right)\right]\Bigg|_{z=z_0} \tag{19}$$

The terms used in Eq. (19) are defined as follows: $V_m(z,t)$ – mean wind speed, spatially averaged (comp. 2.3, Fig. 2), $C_y(z,t)$ – aerodynamic coefficient that depends on W, I_v, L_v and G, f_i – i-th frequency of natural vibrations; φ – shift phase angle.
Non-dimensional vortex excitation can be described by power spectral density function that is, in general, narrow-band Gaussian character and can be given by (comp. Vickery and Clark 1972)

$$\frac{f\cdot G_{\hat{w}_y}(z,f)}{\sigma_{\hat{w}}^2} = \frac{k}{\sqrt{\pi}B}\frac{f}{f_i}\exp\left[-\left(\frac{1-f/f_i}{B}\right)^2\right] \tag{20}$$

where: $\sigma_{\hat{w}}$ – standard deviation of vortex excitation (experimental value); k – factor of the value less than 1.0 (experimental value); B – non-dimensional bandwidth parameter (experimental value); f – frequency.

Eqs (18)-(20) depend explicitly on 4 experimental parameters: α, $\sigma_{\hat{w}}$, k, B. These parameters depend on several wind flow parameters W, I_v, L_v and structure geometry parameters G. Experimental values can be taken for example from: ESDU 80025 (1986), ESDU 82026 (1982), ESDU 85038 (1990).

In particular, the physical meanings of experimental values describing model are as follows:

α – experimental parameter that describes the increase in the effective cross-section diameter. This parameter is connected with the width of the vortex street of the lateral vibrating structure. Its value should be assumed in the range 0.7-1.54 (Flaga 1996, 1997). Variations in the diameter value are considered in Eq. (18) by the factor $\left(1+\alpha\cdot\sigma_{\hat{\eta}}\right)^3$. $\sigma_{\hat{w}}$ – standard deviation of non-dimensional vortex excitation. This parameter depends on the amplitude level of lateral vibrations. In the case when the amplitude vibrations level η exceeds (0.01-0.02)D or standard deviation of lateral displacements σ_η exceeds 0.006D (Kwok and Melbourne, 1980, Vickery and Basu, 1983), considerable amplification of the coefficient $\sigma_{\hat{w}}$ will appear. In literature this value is often identified with the coefficient C_L that describes the whole across-wind load (not only vortex excitation). Values of $\sigma_{\hat{w}}$ can be obtained from the paper by Novak and Tanaka (1977) as the function of lateral vibrations amplitude η. It also can be taken from procedures given in ESDU depending on effective Reynolds number Re_e and surface roughness k_s – ESDU 85038 (1990). k – factor of the value less than 1.0 that takes into account the participation of atmospheric turbulence in the total across-wind load on a structure. The participation of the vortex excitation in the whole across-wind load can be given by the relation: $\sigma_{wv}{}^2 = k \cdot \sigma_{wc}{}^2$, where $\sigma_{wv}{}^2$ – variance of the across-wind load caused by vortex excitation,$\cdot\sigma_{wc}{}^2$ – variance of the whole across-wind load. Mostly, value of k is settled as equal to 1.0, which is not exactly correct, mainly in turbulent flow when vortex excitation can appear in wider range of frequencies. Reduction of the value k below 1.0 was proved in model investigations described by Novak and Tanaka (1977) or Howell and Novak (1980). B – non-dimensional bandwidth parameter. It depends directly on turbulence intensity I_v. If I_v increases, the bandwidth frequency will also increase. Exemplary values were proposed by Novak and Tanaka (1977), Vickery (1995), Basu and Vickery (1983). Vickery's formula: $B = 0.10 + 2I_v$ is accepted in our model.

The fifth experimental parameter of the model is $L_{\hat{w}}$ which has to be calculated in deterministic procedure of $Y(z)$. Value of $L_{\hat{w}}$ depends on non-dimensional amplitude vibrations level $\hat{\eta}$ or standard deviation of non-dimensional amplitudes $\sigma_{\hat{\eta}}$ and can be taken from ESDU 85038 (1990), Ruscheweyh (1989,1992) or codes DIN 1055 (1989) and Eurocode 1 (2009).

In general, in numerical implementation, values of experimental parameters were estimated on the basis of procedures recommended by ESDU.

Summing up, the mathematical model consists of two parts: mathematical and semi-deterministic descriptions. This is a semi-empirical model that depends on five experimental parameters: α, $\sigma_{\hat{w}}$, k, B, $L_{\hat{w}}$.

4. Numerical implementation

4.1. Simulation method

Vortex excitation is a stochastic process and its simulation is based on Weighted Amplitude Waves Superposition method (WAWS). Up to now, this method has been used in order to simulate wind field in many points and in three wind directions. The bases of the method were described by Shinozuka and Jan (1972), Shinozuka (1987), some later modifications and variants were described by Borri (1988), Borri *et al.* (1995), Iannuzzi and Spinelli (1987).

In general, the family of M correlated stochastic processes can be simulated according to the following system of equations

$$p_i(t) = \sum_{k=1}^{N} \sum_{j=1}^{i} H_{ij}(f_k) \cos\Big(2\pi\big(f_k + \delta f_k\big)\big(t + t_{ij}\big) + \Phi_k\Big) \tag{21}$$

A simplified variant of the method is used in our model. Here WAWS method is accepted to direct generation of the equivalent vortex excitation in point z_0. The simulation was performed in one point, because the equivalent load is fully correlated in domain ΔL. The simulation according to the method is based on the knowledge of power spectral density function (PSD), which is given by Eq. (20) and describes the non-dimensional critical vortex excitation. Then, the main simplified equation of WAWS method can be given by

$$p(t) = \sum_{k=1}^{N} \sqrt{2G_i\left(f_k\right)\Delta f_k}\cos\left(2\pi f_k t + \Phi_k\right) \tag{22}$$

There are the following denotations in Eqs (21)-(22): $G_i(f_k)$ – power spectral density function defined by Eq. (20), f_k (k = 1,2....N) – central frequency of frequency interval Δf_k, N – number of spectrum intervals, Φ_k – N random values of phase shift angles taken from the range 0, 2π, $H_{ij}(f_k)$ – expressions of lower-triangle matrix $\mathbf{H}(f_k)$.

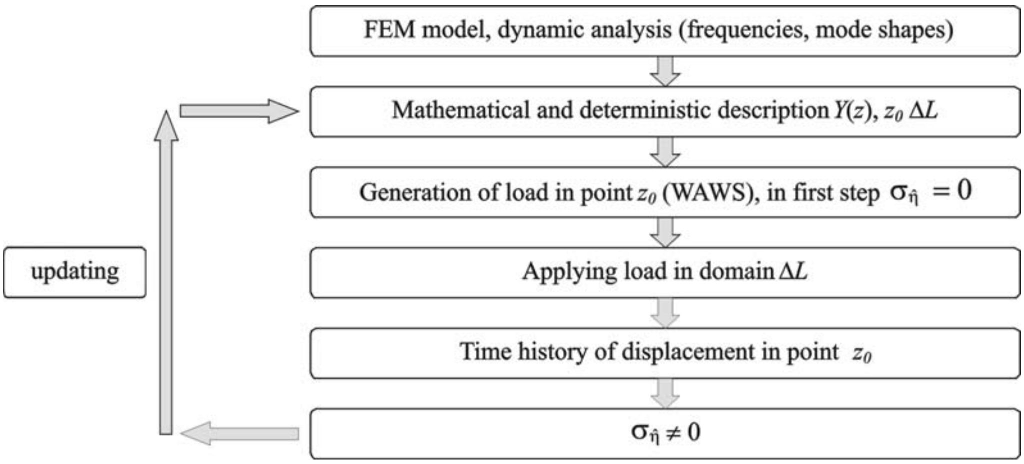

Fig. 9 Computation algorithm

4.2. Simulation procedure

Own computer program "Vortex Load" (based on Finite Element Method program – ALGOR) was created to apply the proposed model. Both across-wind load caused by vortex excitation and lateral response of the analysed structure as well can be generated in time domain. Simplified algorithm of calculations of structure lateral response under vortex excitation is presented in Fig. 9.

The whole simulation procedure can be described in the following steps:

1. FEM discrete model of the structure is created. Frequencies and mode shapes of natural vibrations are obtained as results of modal analysis.

2. Mathematical model parameters (α, $\sigma_{\hat{w}}$, k, $B, L_{\hat{w}}$) are assumed on the basis of wind conditions (e.g., I_v, L_v, $V_m(z)$, etc.). On the other hand the physical description of the wind flow around the structure with regard to vortex excitation zones is performed. Finally, function $Y(z)$, zone (zones) ΔL, and the place of the central point z_0 are determined.

3. A stochastic process of equivalent critical vortex excitation is generated (using WAWS, on the basis of PSD function) in the central point z_0. Then the load is applied to the structure in domain ΔL as a constant value because of full correlation of the process. Firstly, the process is generated in time domain T_0, at each time step Δt taking into account that: $\sigma_{\hat{\eta}} = 0$ (Fig. 10).

4. The time history of displacements in point z_0 and in time domain T_0, at each time step Δt is calculated using direct integration of motion equations (Fig. 11).

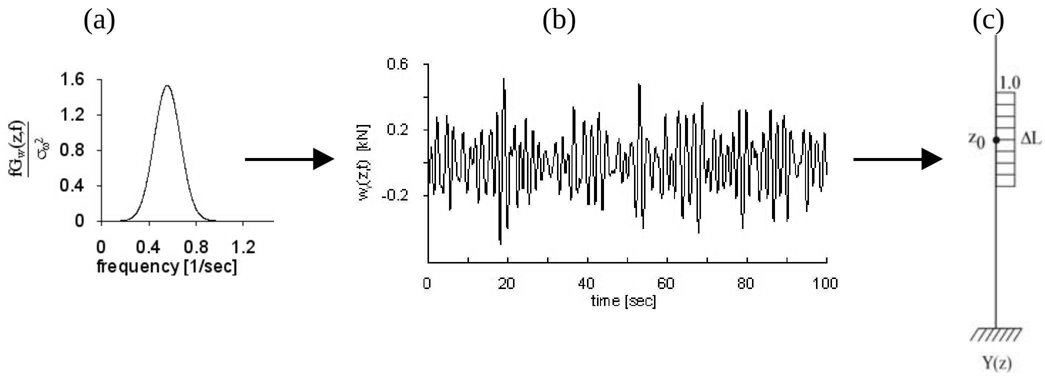

Fig. 10 Load time history simulated with WAWS method (b) on the basis of PSD function (a) and domain ΔL where the load is applied to the structure (c)

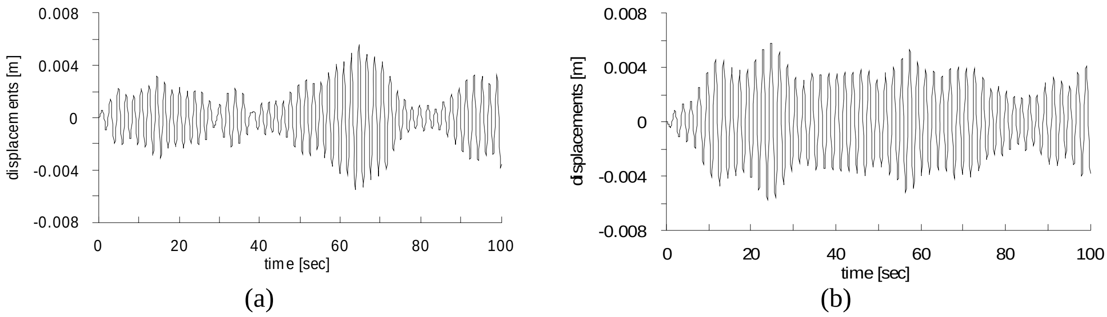

Fig. 11 Two exemplary time histories of displacements for the same simulation parameters: $\sigma_{\hat{\eta}}$ =0, N_t=1000, Δt=0.1s. N_t is the number of time steps Δt

5. A new value of non-dimensional standard deviation of displacements $\sigma_{\hat{\eta}}$ is calculated on the basis of a short time interval in time history of displacements $\chi_1 T_1$, where T_1 – first period of natural vibrations of analysed structure; χ_1 – parameter > 1. Acceptance of χ_1 at low level means that feedback between lateral vibrations and vortex shedding is taken into account. If high value of χ_1 is accepted then feedback is negligible.

Values $Y(z)$, ΔL, z_0 and also Eq. (18) are actualised on the basis of the new $\sigma_{\hat{\eta}}$. Next step(s) of load in time domain (T_0, $T_0 + \Delta\tau$) are generated – Fig. 12. Additional time $\Delta\tau$ contains arbitrary number of time steps Δt.

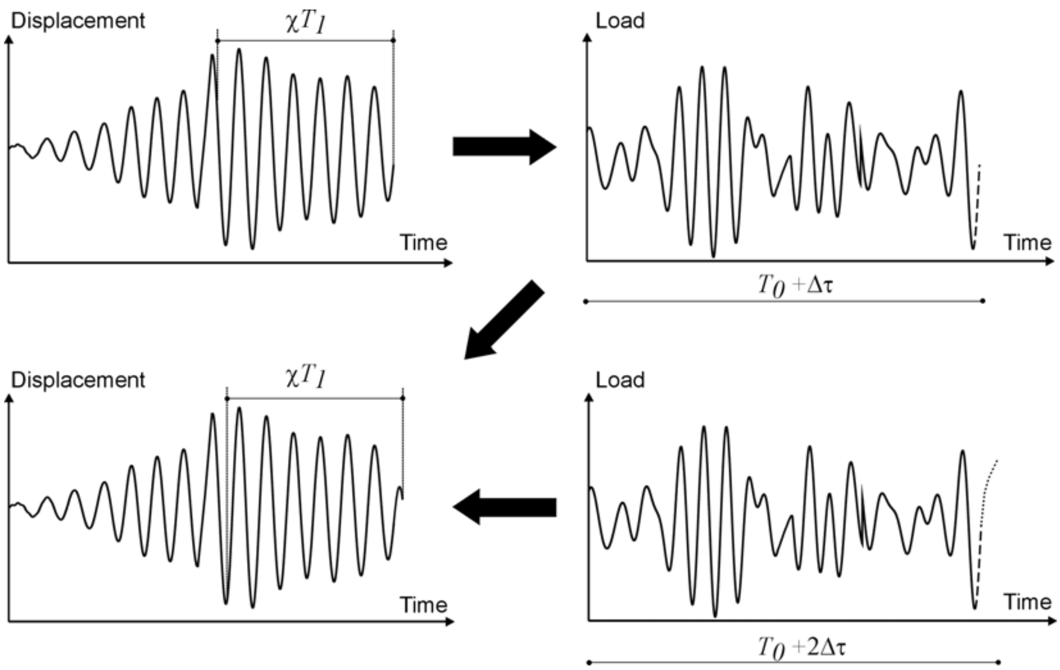

Fig. 12 Load simulation on the basis of time history of displacements in the time interval $\chi_1 T_1$

6. The whole procedure is repeated M times and both time histories of load as well as displacements are obtained in time T ($\sigma_{\hat{\eta}} \neq 0$). So, it can be stated that simulation is performed in time domain (Fig. 13). Further steps of load are simulated using information about displacements before present time.

7. All calculations are repeated N times and then maximum value ($\eta_j^{\max}$) and standard deviation ($\sigma_{\eta j}$) of displacements in time T, in point z_0, in one process and its estimators from N processes (σ_η, η^{max}, g – peak factor) can be obtained according to the following relationships

$$\sigma_{\eta_j} = \sqrt{\frac{1}{T}\int_0^T \left(\eta_j(t) - \bar{\eta}_j\right)^2 dt} = \sqrt{\frac{1}{M}\sum_{i=1}^{M}\left(\eta_{ji} - \bar{\eta}_j\right)^2}, \quad \sigma_\eta = \frac{1}{N}\sum_{j=1}^{N}\sigma_{\eta_j} \tag{23}$$

$$\eta_j^{\max} = \max\left\{\eta_{j,i}\right\}, \qquad \eta^{\max} = \frac{1}{N}\sum_{j=1}^{N}\eta_j^{\max} \tag{24}$$

$$\eta^{\max} = g \cdot \sigma_\eta \tag{25}$$

where: j – index of process, j = 1,2,...N; i – index of predicted discrete value at time $t_i = i\Delta t$ in time interval T, i = 1,2,...,M; $\eta_{ji} = \eta_j(t_i)$ – discrete value of displacements of the j-th process at time t_i.

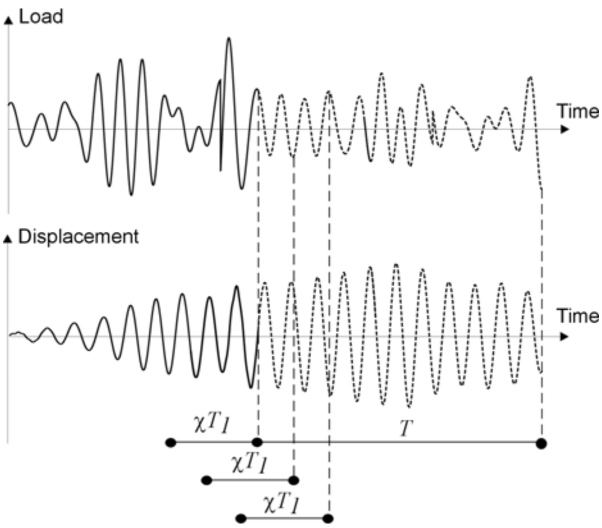

(a)

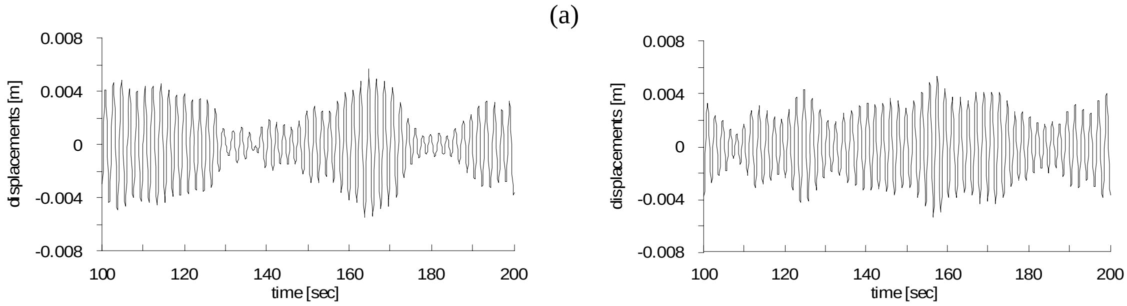

(b)

Fig. 13 Load and displacements time histories in time T, (a) theoretical scheme and (b) real results, for T=100sec, N_t=1000, Δt=0.1s, χ=50, $\Delta\tau=2\Delta t$, 500 repeats (left); T=100sec, N_t=1000, Δt=0.1s, χ=3, $\Delta\tau=\Delta t$, 1000 repeats (right)

5. Conclusions

In authors' opinion the complete description of the vortex excitation phenomenon is contained in the proposed model. This is a semi-empirical model dependent on five experimental parameters (α, $\sigma_{\hat{w}}$, $k, B, L_{\hat{w}}$). It seems that the main difficulties in proper application of the model for slender structures can be encountered at the stage of assuming experimental values. No exact definition or various definitions of coefficients (mainly $\sigma_{\hat{w}}$) are used in literature. It leads to significant discrepancies between the obtained results. The program described here was created for numerical implementation and gives an opportunity to determine vortex excitation as well as structural response in time domain.

References

Arunachalam, S. (2011), "Studies on across-wind load and response of a circular chimney including lock-in effects. Part 1 and part 2", *Proceedings of the 13th International Conference on Wind Engineering*, Amsterdam, Holland.

Basu, R.I. and Vickery, B.J. (1983), "Simplified approaches to the evaluation of the across-wind response of chimneys", *J. Wind Eng. Ind. Aerod.*, **14**, 153-166.

Belver, A.V., Ibán, A.L. and Martin, C.E.L. (2012), "Coupling between structural and fluid dynamic problems applied to vortex shedding in a 90 m steel chimney", *J. Wind Eng. Ind. Aerod.*, **100**, 30-37.

Borri, C., (1988), *Generation procedures of stationary random processes simulating wind time series*, Sezione Strutture 11, Univ. di Firenze.

Borri, C., Crocchini, F., Facchini, L. and Spinelli, P. (1995), "Numerical simulation of stationary and non-stationary stochastic processes: a comparative analysis for turbulent wind fields", *Proceedings of the 9th International Conference on Wind Engineering*, New Delhi, India.

Clobes, M., Willecke, A. and Peil, U. (2011), "Vortex excitation of steel chimneys: Two ultimate limit states", *Proceedings of the 13th International Conference on Wind Engineering*, Amsterdam, Holland.

DIN 1055 (1989), *Lastannahmen für Bauten*, Windwirkungen auf Bauwerke.

ESDU 80025 (1986), *Mean forces, pressures and flow field velocities for circular cylindrical structures: single cylinder with two-dimensional flow*, London, ESDU Int. Ltd.

ESDU 82026 (1982), *Strong winds in the atmospheric boundary layer, Part 1: mean - hourly wind speed*, London, ESDU Int. Ltd.

ESDU 85038 (1990), *Circular-cylindrical structures: dynamic response to vortex shedding, Part I: calculation procedures and derivation*, London, ESDU Int. Ltd.

Eurocode 1 (2009), *Action on structures – part 1-4: General action – Wind action*.

Flaga, A. and Lipecki, T. (2010), "Code approaches to vortex shedding and own model", *Eng. Struct.*, **32**, 1530-1536.

Flaga, A. (1996), *Wind vortex-induced excitation and vibration of slender structures, Single structure of circular cross-section normal to flow*, Monograph 202, Cracow, Poland.

Flaga, A. (1997), "Nonlinear amplitude dependent self-limiting model of lock-in phenomenon at vortex excitation", *J. Wind Eng. Ind. Aerod.*, **69-71**, 331-340.

Flaga, A. and Lipecki, T. (2005), "Simulation of across-wind action caused by vortex excitation", *Proceedings of the 4th European-African Conference on Wind Engineering*, pp. 112-113, Prague, Czech Republic.

Griffin, O.M. and Ramberg, S.E. (1974), "The vortex-street wakes of vibrating cylinders", *J. Fluid Mech.*, **66**(3), 553-576.

Homma, S., Maeda, J. and Hanada, N. (2009), "The damping efficiency of vortex-induced vibration by

tuned-mass damper of a tower-supported steel stack", *Wind Struct.*, **12**(4), 333-348.
Howell, J.F. and Novak, M. (1980), "Vortex shedding from circular cylinders in turbulent flow", *Proceedings of the 5th International Conference on Wind Engineering*, USA 1979, Pergamon, Oxford.
Iannuzzi, A. and Spinelli, P. (1987), "Artificial wind generation and structural response", *J. Struct. Eng.*, **113**(12), 2382-2398.
Kwok, K.C.S. and Melbourne, W.H. (1980), "Cross-wind response of structures due to displacement dependent lock-in excitation", *Proceedings of the 5th International Conference on Wind Engineering*, Colorado, USA, 1979, Pergamon, Oxford, 1980, 699-708.
Novak, M. and Tanaka, H. (1977), "Pressure correlations on a vibrating cylinder", *Proceedings of the 4th International Conference on Wind Effects on Building and Structures*, Heathrow 1975, Cambridge University Press, London.
Repetto, M.P. (2011), "Neutral and non-neutral atmosphere: Probabilistic characterization and wind-induced response of structures", *J. Wind Eng. Ind. Aerod*., **99**, 969-978.
Ruscheweyh, H. (1989), "Codification of vortex excited vibrations. Recent advances in wind engineering", *Proceedings of the 2nd Asia-Pacific Symposium on Wind Engineering*, Beijing, China.
Ruscheweyh, H. (1992), *Windlastannahmen für turmartige Bauwerke, DIN-Mitt*, **71**(11), 644-647, Berlin.
Sachs, P. (1978), *Wind forces in engineering*, Pergamon, Oxford.
Shinozuka, M. and Jan, C.M. (1972), "Digital simulation of random processes and its application", *J. Sound Vib.*, **25**(1), 111-128.
Shinozuka, M. (1987), *Stochastic Mechanics*, Columbia University, NY, USA.
Stansby, P.K. (1976), "Base pressure of oscillating circular cylinders", *Proc. ASCE, J. Eng. Mech. Div.*, **104** (EM 4), 591-600.
Tranvik, P. and Alpsten G. (2005), "Structural behaviour under wind loading of a 90 m steel chimney", *Wind Struct.*, **8**(1), 61-78.
Verboom, G.K. and van Koten H. (2010), "Vortex excitation: Three design rules tested on 13 industrial chimneys", *J. Wind Eng. Ind. Aerod.*, **98**, 145-154.
Vickery, B.J. (1995), *The response of chimneys and tower like structures to wind loading" in "A state of the art in wind engineering*, Wiley Eastern Limited.
Vickery, B.J. and Basu, R.I. (1983), "Across-wind vibrations of structure of circular cross-section", Part 1, *J. Wind Eng. Ind. Aerod.*, **12** (1), 49-74, Part II, *J.Wind Eng. Ind. Aerod.*, **12** (1), 75-98.
Vickery, B.J. and Clark W. (1972), "Lift or across-wind response of tapered stacks", *J. Struct. Eng. Div.-ASCE* , **98**, 1-20.

CC